Axion Physics

Tianjun Li

Institute of Theoretical Physics, Chinese Academy of Sciences

Axion Physics Workshop, IHEP, CAS, June 29, 2020

Outline

Outline

The convincing evidence for physics beyond the SM:

- Dark energy
- Dark matter
- Neutrino masses and mixings
- Baryon asymmetry
- Inflation

The SM is incomplete!

Major Problems in the SM

- Fine-tuning problems
- Aesthetic problems
- Electroweak vacuum stability problem

  It can be solved easily in the new physics models, for example, supersymmetry, etc.

Fine-tuning problems

- Cosmological constant problem

$$\Lambda_{\rm CC} \sim 10^{-122} M_{\rm Pl}^4 ~.$$

- Gauge hierarchy problem

$$M_{\rm EW} \sim 10^{-16} M_{\rm Pl} ~.$$

- Strong CP probelm

$$\theta < 1.3 \times 10^{-10} ~.$$

- The SM fermion masses and mixings

$$m_{\rm electron} \sim 10^{-5} m_{\rm top} ~.$$

Aesthetic Problems:

- Interaction unification
- Fermion unification
- Gauge coupling unification
- Charge quantization
- Too many parameters

These prolems might be solved when we embed the SM into the Grand Unified Theories (GUTs) and string models.

Fine-tuning Problems:

- Cosmological constant problem

  String landscape. Question: how to test it at the future colliders?

- Gauge Hierarchy problem

  Supersymmetry, large extra dimension(s), and strong dynamics, etc.

- Strong CP probelm

  Peccei-Quinn mechanism.

- The SM fermion masses and mixings

  The Froggat-Nielsen meschanism.

String Landscape

- An enormous "landscape" for long-lived metastable string/M theory vacua due to flux compactifications [1].
- Weak anthropic principle [2].
- The first concrete explanation of the very tiny value of the cosmological constant, which can take only discrete values.
- Solution to gauge hierarchy problem.

Although the tiny cosmological constant and light Higgs mass are not technically natural in QFT, they can indeed be natural in the string landscape if the vacua with tiny cosmological constant and light Higgs mass are populated in the string landscape!

The string landscape cannot explain the strong CP problem!

[1] Giddings, Kachru and Polchinski; Kachru, Kallosh, Linde and Trivedi; Susskind; Denef and Douglas.
[2] Weinberg.

Outline

The $U(1)_A$ Problem in the QCD

- The QCD Lagrangian

$$\mathcal{L}_{MSM} = -\frac{1}{2g_s^2}\mathrm{Tr}\, G_{\mu\nu}G^{\mu\nu} + \bar{Q}_i i \not{D} Q_i + \bar{U^c}_i i\not{D} U^c_i + \bar{D^c}_i i\not{D} D^c_i - \left(h_u^{ij} Q_i U^c_j \widetilde{H} + h_d^{ij} Q_i D^c_j H + \mathrm{H.C.}\right) .$$

The $U(1)_A$ Problem in the QCD

- Because $m_u/m_d << \Lambda_{QCD}$, we have approximate $U(2)_V \times U(2)_A$ symmetry.
- $U(2)_V = SU(2)_I \times U(1)_B$ is a good approximate symmetry of nature.
- Quark condensations $\langle \bar{u}u \rangle / \langle \bar{d}d \rangle \neq 0$ break the $U(2)_A$ symmetry, so we have four Nambu-Goldstone bosons.
- Although pions are light, we do not have another light state due to $\left(m_{\eta'} \simeq 960 \text{ MeV}\right)^2 >> \left(m_\pi^2 \simeq 140 \text{ MeV}\right)^2$.

$U(1)_A$ **is not a symmetry in QCD.**

The Solution to the $U(1)_A$ Problem

- The topological term

$$\mathcal{L}_\theta = \frac{\theta}{16\pi^2} \mathrm{Tr} F^{\mu\nu} \widetilde{F}^{\mu\nu} , \quad \widetilde{F}^{\mu\nu} = \frac{1}{2} \epsilon^{\mu\nu\alpha\beta} F_{\alpha\beta} .$$

- The topological term is a total derivative

$$F_{\mu\nu} \widetilde{F}^{\mu\nu} = \partial_\mu K_\mu, \; K_\mu = \frac{1}{16\pi^2} \epsilon^{\mu\nu\alpha\beta} \left(A^a_\nu \partial_\alpha A^a_\beta + \frac{1}{3} f_{abc} A^a_\nu A^b_\alpha A^c_\beta \right) .$$

- Being a total derivative, the θ term does not affect the equations of motion.

The Solution to the $U(1)_A$ Problem

- The field configurations with the instanton boundary conditions give rise to a nonvanishing

$$\int d^4x (\mathcal{L}_\theta)_{\text{one instanton}} = \theta \ .$$

- $\mathcal{L}_\theta$ is not $U(1)_A$ invariant, and then $U(1)_A$ is not a symmetry of QCD

Two Higgs doublets are needed for the $U(1)_A$ invariance for the Yukawa couplings

$$q_f \longrightarrow e^{i\gamma_5 \alpha} q_f \ , \quad \theta \longrightarrow \theta - 2\alpha \ .$$

Strong CP Problem

- $\overline{\theta} = \theta + \theta_{\rm q}$ parameter is a dimensionless coupling constant and infinitely renormalized by radiative corrections.

$$\theta_{\rm q} \;=\; {\rm ArgDet}(Y_U Y_D)\ .$$

- The experimental bound on the neutron EDM is smaller than 3.0×10^{-26} e cm, while the contribution from the $\bar{\theta}$ is

$$d_n \;=\; 2.4(1.0)^{-16}\overline{\theta}\ {\rm e\ cm}\ .$$

- No theoretical reason for $\overline{\theta}$ as small as 10^{-10} required by the experimental bound on the EDM of the neutron.
- $\overline{\theta}$ may be a random variable with a roughly uniform distribution in the string landscape.

Strong CP problem: why $\overline{\theta}$ is so tiny?

The Possible Solutions to the Strong CP Problem

- Massless quark solution, but not consistent with Lattice QCD.

  If one of the quark fields (say the up quark) was massless, the QCD Lagrangian would have a global $U(1)_u$ axial symmetry, which could be used to rotate the $\overline{\theta}$ term to zero.

- RGE running of $\overline{\theta}$: $\overline{\theta}$ is chosen to be zero at some high scale.

  We can show that all 6-loop diagrams and below cannot generate any RG running.

- Parity: $\overline{\theta} = \theta + \mathrm{ArgDet}(Y_u) + \mathrm{ArgDet}(Y_d) = 0$

  $$P : SU(2)_L \leftrightarrow SU(2)_R \,,\; Q_L \leftrightarrow Q_R^{\dagger} \,,\; H_L \leftrightarrow H_R^{\dagger} \,,\;\; L_L \leftrightarrow L_R^{\dagger} \,.$$

  θ is forbidden, and Y_u/Y_d are Hermitian. The problem arises after a bi-fundamental Higgs is added due to the one-loop contribution to $\overline{\theta}$.

- Soft P (CP) breaking typically called Nelson-Barr models.

  CP is a valid symmetry in the high-energy theory, and is spontaneously broken in such a way that θ naturally turns out to be small. The fine-tuning is still needed.

Peccei–Quinn Mechanism

- The $U(1)_A$ symmetry becomes $U(1)_{PQ}$ symmetry.
- If there are two Higgs doublets in the SM, we can have the $U(1)_{PQ}$ symmetry [3]

$$
\begin{aligned}
-\mathcal{L} &= y^u_{ij} Q_i U^c_i H_u + y^d_{ij} Q_i D^c_i H_d + y^e_{ij} L_i E^c_i H_d \\
&\quad + V\left(H_u^\dagger H_u,\ H_d^\dagger H_d,\ (H_d^\dagger H_u)(H_u^\dagger H_d)\right) ~.
\end{aligned}
$$

- The $U(1)_{PQ}$ symmetry

$$
\begin{aligned}
& Q_i/U^c_i/D^c_i/L_i/E^c_i \longrightarrow e^{i\alpha} Q_i/U^c_i/D^c_i/L_i/E^c_i ~, \\
& H_d/H_u \longrightarrow e^{-i2\alpha} H_d/H_u ~.
\end{aligned}
$$

[3] Weinberg; Wilczek.

Peccei–Quinn-Weinberg-Wilczek Axion

- Peccei–Quinn-Weinberg-Wilczek Axion is

$$a \equiv \sin\beta \mathrm{Im} H_d^0 + \cos\beta \mathrm{Im} H_u^0 ~, \quad \mathrm{where} \tan\beta \equiv \frac{\langle H_u^0\rangle}{\langle H_d^0\rangle} ~.$$

- The solution to the strong CP problem: $\overline{\theta} = 0$.

$$V_{\rm Instanton} ~=~ -m_\pi^2 f_\pi^2 \sqrt{1 - \frac{4 m_u m_d}{(m_u+m_d)^2} \sin^2\left(\frac{\overline{\theta}}{2}\right)} ~,$$

$$\overline{\theta} = \theta + \theta_{\rm q} + a/f_a ~, \quad f_a = \sqrt{\langle H_u^0\rangle^2 + \langle H_d^0\rangle^2} ~.$$

- The axion mass

$$m_a ~=~ \frac{m_\pi f_\pi}{f_a} \frac{\sqrt{m_u m_d}}{m_u + m_d} \sim 5.7 \left(\frac{10^{12}~\mathrm{GeV}}{f_a}\right) \mu\mathrm{eV} ~.$$

Peccei–Quinn-Weinberg-Wilczek Axion

- Weak axion, which has $f_a \sim 246$ GeV and $m_a \sim 25$ keV, is ruled out by $K \to \pi a$ and $J/\Psi \to a\gamma$ experiments.
- Question: can we propose the axion models with the TeV-scale $U(1)_{PQ}$ symmetry breaking and very large f_a?
- Answer: No!
- Point: anomaly argument, and then the only relevant parameter is f_a.
- Solutions: invisible DFSZ and KSVZ Axions

Introducing a SM singlet S with intermediate-scale VEV, so $f_a \simeq \langle S \rangle \simeq 10^{10} - 10^{12}\mathrm{GeV}$.

The DFSZ Axion

- The PQWW model with an SM singlet S

$$S \longrightarrow e^{i2\alpha} S ~, ~~~ -\mathcal{L} = S^2 H_d H_u ~.$$

- In the supersymmetric SMs, we have

$$W ~~=~~ \frac{1}{M_{\rm Pl}} S^2 H_d H_u ~.$$

  A natural solution to the μ problem.

- The DFSZ Axion

$$a \equiv \frac{1}{f_a} \left(\langle H_u^0 \rangle {\rm Im} H_d^0 + \langle H_d^0 \rangle {\rm Im} H_u^0 + \langle S \rangle {\rm Im} S \right) ~.$$

where $f_a = \sqrt{\langle H_u^0 \rangle^2 + \langle H_d^0 \rangle^2 + \langle S \rangle^2}$.

The KSVZ Axion

- A pair of vector-like quarks (XQ^c, XQ) and a SM singlet S

$$XQ^c/XQ \longrightarrow e^{i\alpha}XQ^c/XQ~, \quad S \longrightarrow e^{-i2\alpha}S~.$$

- The Lagrangian is

$$-\mathcal{L} = SXQ^cXQ~.$$

- The KSVZ axion is the imaginary part of S, and $f_a = |\langle S \rangle|$.

The Minimal Invisible Axion Model [4]

- The SM with a SM singlet S, and the $U(1)_{PQ}$ charges are

$$Q_i,\ L_i,\ U_i^c,\ D_i^c, E_i^c : 1\ ,\quad H_u : 2\ ,\quad S : -4\ .$$

- The Lagrangian is

$$\mathcal{L} \quad = \quad -y_{ij}^u Q_i U_j^c H_u - y_{ij}^d \frac{S}{M_*} Q_i D_j^c \widetilde{H}_u, -y_{ij}^e \frac{S}{M_*} L_i E_j^c \widetilde{H}_u\ .$$

- For M_* to be the reduced Planck scale, the effective axion PQ scale will be $f_a \sim 10^{15-16}$ GeV.

[4] Y. Gao, T. Li and Q. Yang, [arXiv:1912.12963 [hep-ph]].

Axion Dark Matter Relic Density

- Axion dark matter density is

$$\Omega_a h^2 = 0.15X \left(\frac{f_a}{10^{12}\,\mathrm{GeV}} \right)^{7/6} .$$

- Pre-inflationary scenario: misalignment mechanism, and $X \sim \sin^2 \theta_{\rm miss}/2$.
- Post-inflationary scenario: misalignment mechanism and topological defect decays, and $X \subset (2, 10)$.

Topological defects are mainly strings and domain walls associated with the axion field.

- Axion dark matter density is [5]

$$\Omega_a h^2 \simeq 0.12 \left(\frac{28\,\mu\mathrm{eV}}{m_a} \right)^{7/6} = 0.12 \left(\frac{f_a}{2.0 \times 10^{11}\,\mathrm{GeV}} \right)^{7/6} .$$

[5] L. Di Luzio, M. Giannotti, E. Nardi and L. Visinelli, [arXiv:2003.01100 [hep-ph]].

Axion Mass

- The axion mass is [6]

$$m_a \simeq 5.70(7)\,\mu\mathrm{eV}\left(\frac{10^{12}\,\mathrm{GeV}}{f_a}\right) .$$

- The more previse calculations give $m_a = 60 - 150\ \mu\mathrm{eV}$ [7], and $m_a = 26.5 \pm 3.4\ \mu\mathrm{eV}$ [8].
- The axion mass is around 50 $\mu\mathrm{eV}$.

[6] G. Grilli di Cortona, E. Hardy, J. Pardo Vega and G. Villadoro, JHEP **01**, 034 (2016).

[7] T. Hiramatsu, M. Kawasaki, K. Saikawa and T. Sekiguchi, Phys. Rev. D **85**, 105020 (2012); M. Kawasaki, K. Saikawa and T. Sekiguchi, Phys. Rev. D **91**, no.6, 065014 (2015).

[8] V. B. Klaer and G. D. Moore, JCAP **11**, 049 (2017).

The Axion Lagrangian

$$\mathcal{L}_a^{\rm int} \supset \frac{\alpha}{8\pi}\frac{C_{a\gamma}}{f_a} aF\tilde{F} + C_{af}\frac{\partial_\mu a}{2f_a}\bar{f}\gamma^\mu\gamma_5 f + \frac{C_{a\pi}}{f_a f_\pi}\partial_\mu a[\partial\pi\pi\pi]^\mu - \frac{i}{2}\frac{C_{an\gamma}}{m_n}\frac{a}{f_a}\bar{n}\sigma_{\mu\nu}\gamma_5 n F^{\mu\nu} ,$$

where $[\partial\pi\pi\pi]^\mu = 2\partial^\mu\pi^0\pi^+\pi^- - \pi_0\partial^\mu\pi^+\pi^- - \pi_0\pi^+\partial^\mu\pi^-$,

The Axion Lagrangian

$$
\begin{aligned}
C_{a\gamma} &= \frac{E}{N} - 1.92(4)\,, \\
C_{ap} &= -0.47(3) + 0.88(3)\, c_u^0 - 0.39(2)\, c_d^0 - C_{a,\,\mathrm{sea}}\,, \\
C_{an} &= -0.02(3) + 0.88(3)\, c_d^0 - 0.39(2)\, c_u^0 - C_{a,\,\mathrm{sea}}\,, \\
C_{a,\,\mathrm{sea}} &= 0.038(5)\, c_s^0 + 0.012(5)\, c_c^0 + 0.009(2)\, c_b^0 + 0.0035(4)\, c_t^0\,, \\
C_{ae} &= c_e^0 + \frac{3\alpha^2}{4\pi^2}\left[\frac{E}{N}\log\left(\frac{f_a}{m_e}\right) - 1.92(4)\log\left(\frac{\mathrm{GeV}}{m_e}\right)\right]\,, \\
C_{a\pi} &= 0.12(1) + \frac{1}{3}\left(c_d^0 - c_u^0\right)\,, \\
C_{an\gamma} &= 0.011(5)\, e\,.
\end{aligned}
$$

The Axion Lagrangian

$$\mathcal{L}_a^{\rm int} \supset \frac{1}{4} g_{a\gamma} a F \tilde{F} - i g_{af} a \bar{f} \gamma_5 f - \frac{i}{2} g_d \, a \, \bar{n} \sigma_{\mu\nu} \gamma_5 n F^{\mu\nu} \, , .$$

where

$$g_{a\gamma} = \frac{\alpha}{2\pi} \frac{C_{a\gamma}}{f_a} \, , \qquad g_{af} = C_{af} \frac{m_f}{f_a} \, , \qquad g_d = \frac{C_{an\gamma}}{m_n f_a} \, .$$

Axion Electrodynamics:

- Generic coupling to electromagnet field:

$$\mathcal{L} = -\frac{1}{4}F_{\mu\nu}F^{\mu\nu} - J^{\mu}A_{\mu} + \frac{1}{2}\partial_{\mu}a\partial^{\mu}a - \frac{1}{2}m_a^2a^2 - \frac{1}{4}g_{a\gamma\gamma}aF_{\mu\nu}\tilde{F}^{\mu\nu}$$

$g_{a\gamma\gamma} = \frac{\alpha g_{\gamma}}{\pi f_a}$

Modified Maxwell's Equations:

- $\nabla \times \vec{B} - \frac{\partial \vec{E}}{\partial t} = \vec{j} + g_{a\gamma\gamma}(\vec{B}\frac{\partial a}{\partial t} - \vec{E} \times \nabla a)$
- $\nabla \cdot \vec{E} = \rho - g_{a\gamma\gamma}\vec{B} \cdot \nabla a$
- $\nabla \cdot \vec{B} = 0$
- $\nabla \times \vec{E} + \frac{\partial \vec{B}}{\partial t} = 0$

$$\partial_{\mu}F^{\mu\nu} = j^{\nu} - g_{a\gamma\gamma}\tilde{F}^{\mu\nu}\partial_{\mu}a$$

Axion current: $J_a^{\nu} \equiv -g_{a\gamma\gamma}\tilde{F}^{\mu\nu}\partial_{\mu}a$

Bianchi identity: $\partial_{\mu}\tilde{F}^{\mu\nu} = 0$

$\nabla a \sim 0$ (Gradients suppressed by $V_{\rm DM} \sim 10^{-3}$)

The Axion Quality Problem

- Because $U(1)_{PQ}$ symmetry is an anomalous symmetry, we cannot forbid the terms such as MXQ^cXQ and $M_S^2S^2$, etc, w hich breaks the $U(1)_{PQ}$ symmetry, for the EFT point of view.
- The global symmetries will be broken by quantum gravity effect. Let us consider the following set of effective operators of dimension $d = 2m + n$ that violate the PQ symmetry by n units

The Axion Quality Problem

$$V^n_{\rm PQ-break} = \frac{\lambda_n |\Phi|^{2m}\left(e^{-i\delta_n}\Phi^n + e^{i\delta_n}{\Phi^\dagger}^n\right)}{{\rm M_{Pl}}^{d-4}}$$
$$\supset \frac{\lambda_n f_a^4}{2}\left(\frac{f_a}{\sqrt{2}{\rm M_{Pl}}}\right)^{d-4} \cos\left(\frac{na}{f_a} - \delta_n\right)$$
$$\approx m_*^2 f_a^2 \left(\frac{\theta^2}{2} - \frac{\theta}{n}\tan\delta_n\right) ,$$

where $m_*^2 = \frac{\lambda_n f_a^2}{2}\left(f_a/(\sqrt{2}{\rm M_{Pl}})\right)^{d-4}\cos\delta_n$.

The Axion Quality Problem

- The CP conserving minimum $\theta = 0$ of the QCD induced potential is shifted to

$$\langle\theta\rangle = \frac{m_*^2 \tan\delta_n}{n(m_a^2 + m_*^2)} .$$

- To satisfy the neutron EDM constraint, we require $d \geq 8, 10, 21$ respectively for $f_a \sim 10^8, 10^{10}, 10^{15}$ GeV.
- Solution: the anomalous $U(1)_X$ gauge symmetry in string models which is broken down to the discrete Z_N symmetry, etc.

The Connections between Axion/ALP and New Physics

- The supersymmetric SMs: μ problem, dark matter density problem, etc.
- The Grand Unified Theories.

  There exists the possibility: no coupling between axion and photons.
- The superstring models: many Axion-Like Particles (ALPs).

  Witten, Axions may be intrinsic to the structure of string theory.
- Axion inflation.
- The intermediate-scale coincidence: the $U(1)_{PQ}$ symmetry breaking scale, right-handed neutrino masses, supersymmetry breaking scale, messenger scale in gauge mediation, axion quality problem, and string-scale gauge coupling unification, etc.
- Relaxation mechanism

  Solutions to the gauge hiearchy problem, etc.

The Connections between Axion/ALP and New Physics

- Dark matter.
- Dark energy particles are similar to axion/ALPs.

  Quintessence Field, Chameleons, Galileons, and Symmetrons, etc.
- Baryon asymmetry via axion quark nugget (AGN).
- The Froggatt-Nielsen (FN) mechanism is the solution to the fermion mass hierarchy problem: $U(1)_{FN} = U(1)_{PQ}$.
- Gravitational wave:

  $\frac{\alpha_g}{4} a R^{\beta}{}_{\alpha\gamma\delta} \tilde{R}^{\alpha}{}_{\beta}{}^{\gamma\delta}$ with $\tilde{R}^{\alpha}{}_{\beta}{}^{\gamma\delta} \equiv \frac{1}{2}\epsilon^{\gamma\delta\mu\nu} R^{\alpha}{}_{\beta\mu\nu}$.
- The neutrino masses and mixings: $U(1)_{BL} = U(1)_{PQ}$, and the baryon asymmetry can be explained via the leptogenesis.
- The EDGES results and XENON1T results, etc.

Outline

Introduction and Motivation

Strong CP Problem and Peccei–Quinn Mechanism

Axion Experiments

Explanation of the XENON1T Excess via Axion

Detection of axion/ALP

The various axion searches can be categorized by if the axion is dark matter.

1.Dark Matter independent searches

Axion from natural sources:

Axion helioscopes(CAST,IAXO)

Underground Detectors(XENON,PANDAX,LUX)

Cherenkov Telescopes(AS-γ,LHAASO,HESS)

Producing axion/ALPs in the lab:

Light shining through walls (ALPS(I-III))

Fifth force experiments(ARIADNE,QUAX)

Polarization experiments(PVLAS)

Solar Axion (CAST,IAXO)

Latest CAST limit: $g_{a\gamma} < 0.66 \times 10^{-10}\mathrm{GeV}^{-1}$at 95%CL

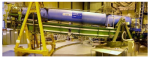
CAST at CERN

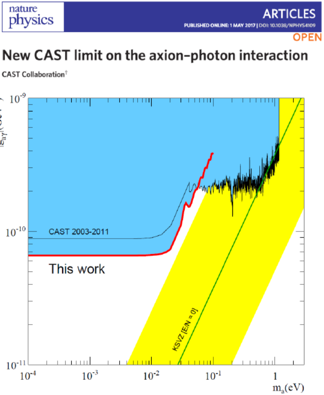
nature physics ARTICLES
PUBLISHED ONLINE: 1 MAY 2017 | DOI: 10.1038/NPHYS4109
OPEN

New CAST limit on the axion–photon interaction

CAST Collaboration†

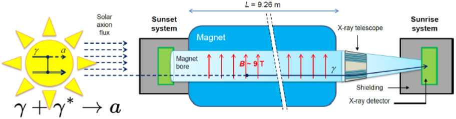

$\gamma + \gamma^* \to a$

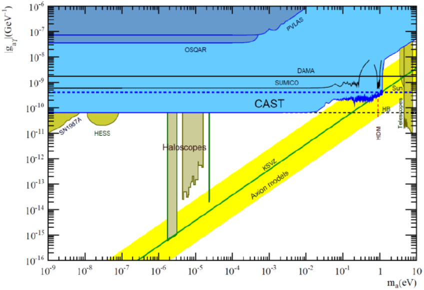

In the future, IAXO

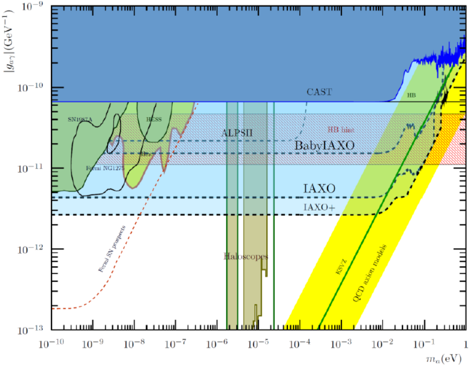

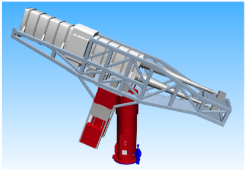

Baby IAXO
(Intermediate experimental stage before IAXO)

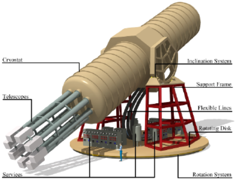

IAXO

Solar Axion: direct detection experiment
Underground Detectors(XENON,PANDAX,LUX)

Due to the coupling of Axion to electron and nucleon, the solar Axion with high energy can generate recoil signal in low temperature dark matter detector.

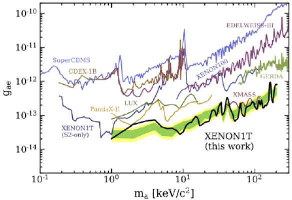

XENON Collaboration
arXiv:2006.0972

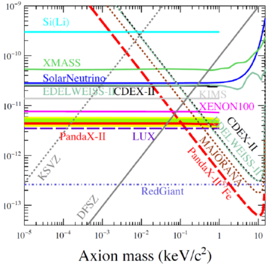

PANDAX, Collaboration
PRL 119 (2017)

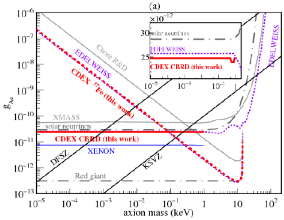

CDEX, Collaboration
Phys.Rev. D95
(2017) no.5, 052006

HE photon energy spectrum:

High Energy photons traversing in stellar or interstellar magnetic fields could convert into axion, resulting in the distortion of photon energy spectrum:

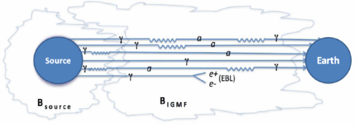

$$P_{\gamma\to a}(E_\gamma) = \left(1+\frac{E_c^2}{E_\gamma^2}\right)^{-1}\sin^2\left(\frac{g_{a\gamma\gamma}B_{\rm T}L}{2}\sqrt{1+\frac{E_c^2}{E_\gamma^2}}\right)$$

Gama ray telescopes like AS-γ,LHAASO,HESS can observe HE photons from very distant sources:

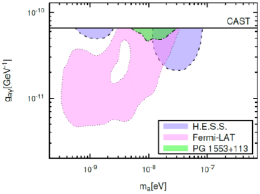

J.Guo, H.-J. Li, X.-J. Bi,
S.-J. Lin, P.-F. Yin 2002.07571

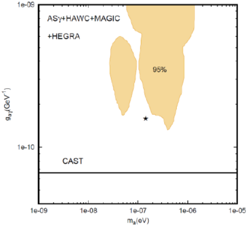

AS-γ轴子限制：X.-J.Bi, Y.Gao, J.Guo,
N.Houston, T. Li, F.Xu, X.Zhang, 2002.01796

Light-shining-through-wall(LSW) (ALPS,OSQAR)

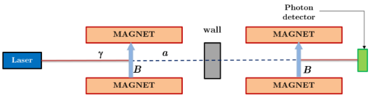

Standard LSW experiment configuration

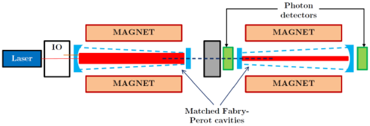

Enhanced LSW configuration (future)

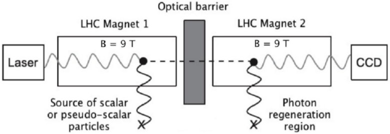

FIG. 1. Principle of the OSQAR LSW experiment.

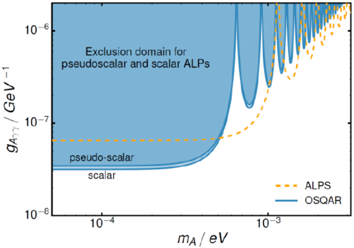

OSQAR: Phys.Rev.Lett. 113 (2014) no.16, 161801
ALPS: Phys.Lett. B689 (2010) 149-155

Polarization experiments(PVLAS)

PVLAS experiment: study QED vacuum birrefringence and sensitivty to ALPs:

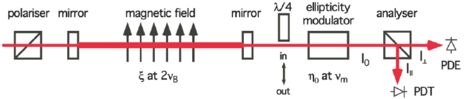

Dichroism:
Production of real particles

Ellipticity:
Production of massive virtual particles

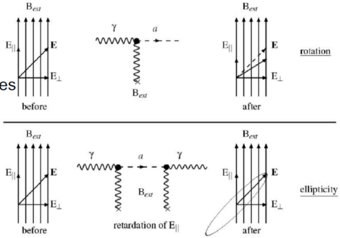

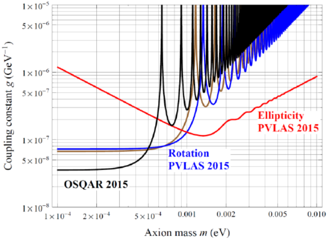

PVLAS , EPJC 76 (2016) no.1, 24

Axion-mediated macroscopic forces

If $\bar{\theta} \neq 0$, the axion has a coupling: $\bar{\theta}\psi\bar{\psi}am_{\psi}/f$. It will mediate a $\bar{\theta}^{2}/f^{2}r^{2}$ force.

If the axion has spin couplings: $\bar{\psi}\gamma^{\mu}\gamma^{5}\psi\partial_{\mu}a/f$ .It will mediate a $1/f^{2}r^{4}$ force between spins.

If it has both of these couplings, then there is also a $\bar{\theta}/f^{2}r^{3}$ force between the two objects.

The concomitant interactions between fermions mediated by ALP exchange are of three types:

1.Monopole-Monopole $\propto \bar{g}_{a\psi}\bar{g}_{a\psi'}$

2.Monopole-Dipole $\propto \bar{g}_{a\psi}g_{a\psi'}$

3.Dipole-Dipole $\propto g_{a\psi}g_{a\psi'}$

ARIADNE experiment

Search the short-range force by NMR technique, the experiment is sensitive to products of fermion couplings: $\propto \bar{g}_{a\psi} g_{a\psi'}$

Arvanitaki, Geraci
Phys. Rev. Lett. 113, 161801 (2014)

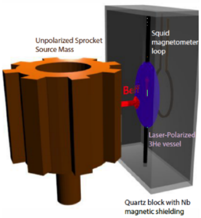

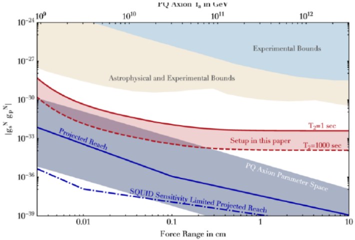

QUAX experiment

Search the monopole-dipole force coupled to electron-spins $\propto \bar{g}_{aN} g_{ae}$ by detecting the magnetization induced by a extra magnet field(created by the axion field gradient) in a paramagnetic material

N. Crescini, C. Braggio, et al
, Nucl. Instrum. Meth. A842 (2017) 109–113

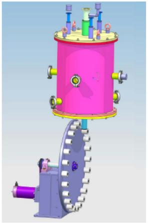

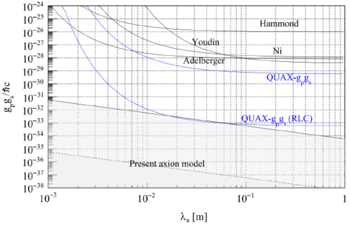

2.Axion Dark Matter searches
(Searches for axions/ALPs that rely on them being dark matter)

DM-photon conversions in the lab:

Conventional Haloscopes(ADMX, HAYSTAC, ORGAN,CAPP-CULTASK,CAST-CAPP)

Dielectric Haloscopes(MADMAX)

Low frequency resonators with LC circuits (ABRACADABRA)

DM induced Oscillating EDMs:

NMR techniques(CASPER)

Low frequency resonators with LC circuits (ABRACADABRA)

ABRACADABRA at MIT

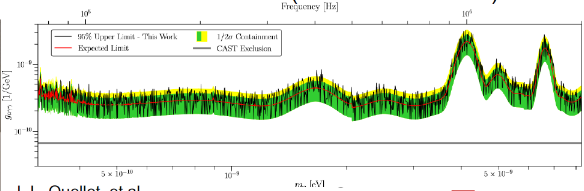

J. L. Ouellet, et.al.
Phys. Rev. Lett. **122**, 121802(2019)

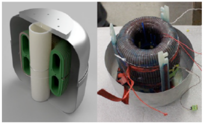

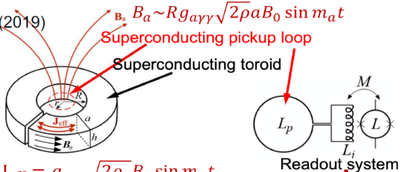

$B_a \sim R g_{a\gamma\gamma}\sqrt{2\rho_a}B_0 \sin m_a t$

$\mathrm{J_{eff}} = g_{a\gamma\gamma}\sqrt{2\rho_a}B_0 \sin m_a t$

$\Phi_a(t) = g_{a\gamma\gamma}\sqrt{2\rho a}B_0 \sin m_a t \times B_0 V G_{toroid}$

$f_a = 10^{16} GeV, B_0 \sim 5T$, R$\sim 4m$: $B_a \sim 10^{-22} T (KSVZ)$

DM induced Oscillating EDMs: NMR techniques(CASPER)

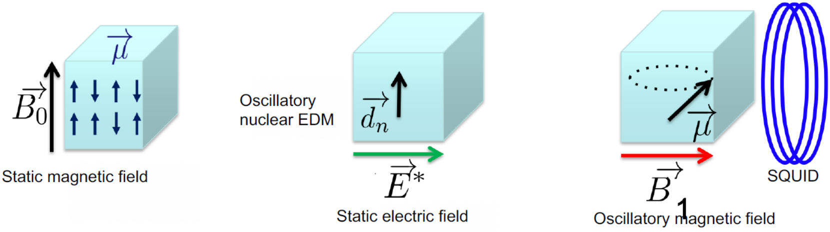

The applied magnetic field is colinear with the sample magnetization.

The effective electric field in the crystal is perpendicular to the applied magnetic field.

The SQUID pickup loop is arranged to measure the transverse magnetization of the sample.

PRD 88 (2013) arXiv:1306.6088, PRX (2014) arxXiv:1306.6089, PRD 84 (2011) arXiv:1101.2691

Nuclear Spin Precession in Electric and Magnetic Fields (nEDM)

Due to the periodic oscillation of the Axion field, the neutrons (nuclei) obtain periodic EDM

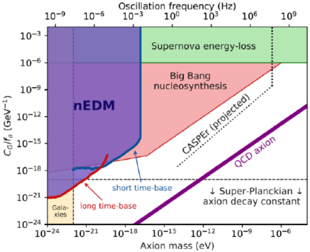

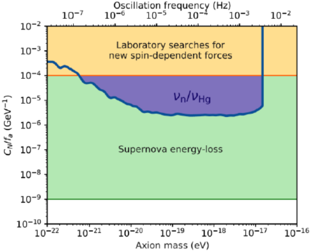

C. Abel,et al. PRX7 (2017) no.4, 041034

$$d_n(t) \approx +2.4 \times 10^{-16}\, \frac{C_G a_0}{f_a} \cos(m_a t)\ e \cdot \mathrm{cm}$$

$$H_{\rm int}(t) = \frac{C_N a_0}{2 f_a} \sin(m_a t)\ \boldsymbol{\sigma}_N \cdot \boldsymbol{p}_a$$

$$d_{\rm Hg}(t) \approx +1.3 \times 10^{-19}\, \frac{C_G a_0}{f_a} \cos(m_a t)\ e \cdot \mathrm{cm}$$

Dielectric Haloscopes(MADMAX)

DM field + Magnet field + Boundary condition in the dish
Theory predicts that there will be photon emission normal to surface

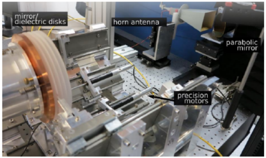

MADMAX at DESY

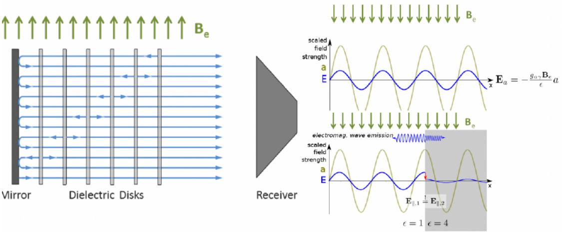

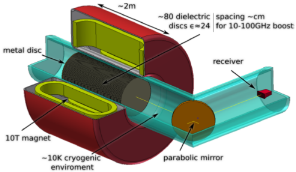

To satisfy the usual continuity requirements:
$\boldsymbol{E}_{\parallel,1} = \boldsymbol{E}_{\parallel,2}$ and $\boldsymbol{B}_{\parallel,1} = \boldsymbol{B}_{\parallel,2}$,EM waves of frequency:$\nu_a = m_a/2\pi$ must be present to compensate for the discontinuity

Haloscopes(Resonant Cavity experiment)

ADMX HAYSTAC CAPP-CULTASK

Resonant cavity detection is one of prevalent and mature scheme

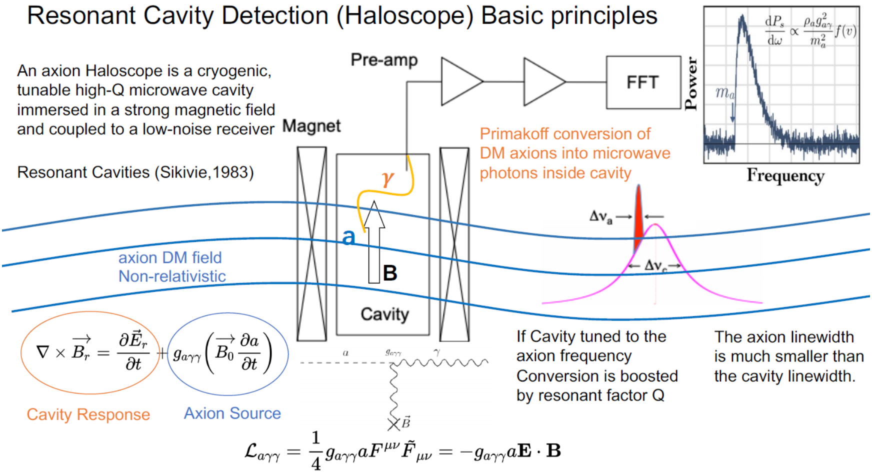
Resonant Cavity Detection (Haloscope) Basic principles
An axion Haloscope is a cryogenic, tunable high-Q microwave cavity immersed in a strong magnetic field and coupled to a low-noise receiver
Resonant Cavities (Sikivie,1983)
Pre-amp
FFT
Power
Frequency
m_a
$\frac{dP_s}{d\omega} \propto \frac{\rho_a g_{a\gamma}^2}{m_a^2} f(v)$
Magnet
Primakoff conversion of DM axions into microwave photons inside cavity
γ
a
B
Cavity
axion DM field
Non-relativistic
Δv_a
Δv_c
$\nabla \times \vec{B}_r = \frac{\partial \vec{E}_r}{\partial t} + g_{a\gamma\gamma}\left(\vec{B}_0 \frac{\partial a}{\partial t}\right)$
Cavity Response
Axion Source
If Cavity tuned to the axion frequency Conversion is boosted by resonant factor Q
The axion linewidth is much smaller than the cavity linewidth.
$\mathcal{L}_{a\gamma\gamma} = \frac{1}{4} g_{a\gamma\gamma} a F^{\mu\nu} \tilde{F}_{\mu\nu} = -g_{a\gamma\gamma} a \mathbf{E} \cdot \mathbf{B}$

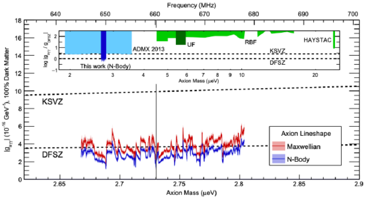

ADMX Collaboration Phys. Rev. Lett. 120, 151301(2018)

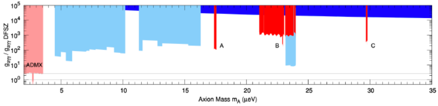

ADMX sidecar experiment(Higher-m_a experiment)
ADMX Collaboration Phys. Rev. Lett. 121, 261302(2019)

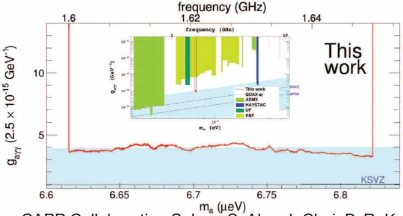

CAPP Collaboration S. Lee, S. Ahn, J. Choi, B. R. Ko, and Y. K. Semertzidis Phys. Rev. Lett. **124**, 101802 (2020)

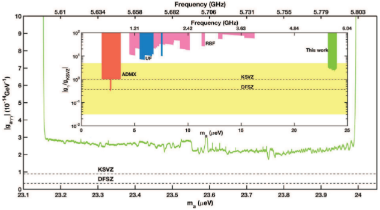

L. Zhong et al., Phys. Rev. D 97, 092001 (2018)

Overall picture(Constraints and Future constraints for $g_{a\gamma}$)

There are already many constraints on axion physics, and many experiments planning to search even further
At present, only the resonant cavity experiment can directly test the theoretical accuracy of QCD axion

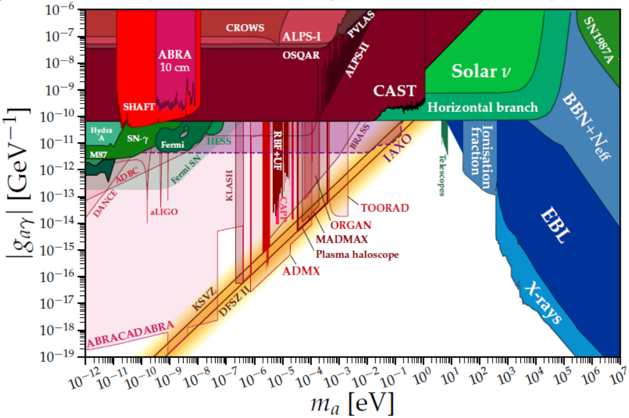

Our proposal:

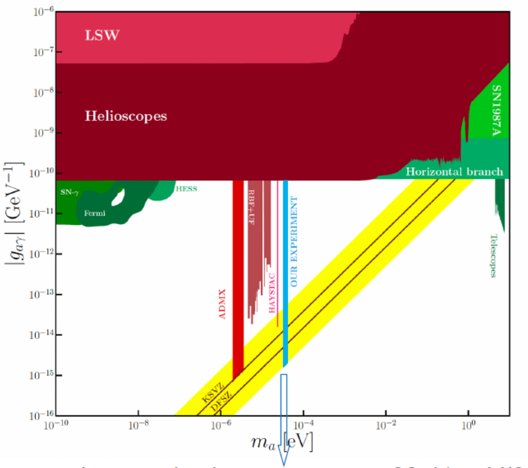

Oure goal covered axion mass range~32-41 μeV(8-10GHz)

Our proposal:

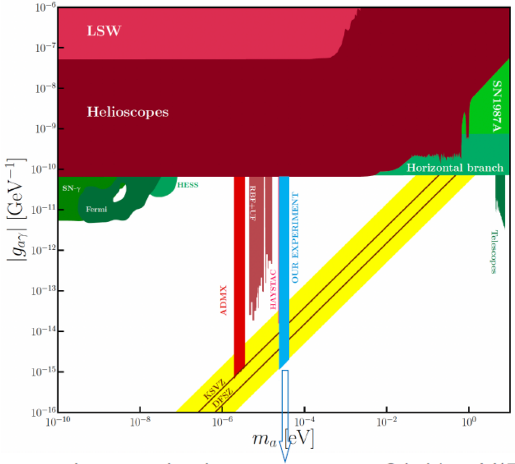

Oure goal covered axion mass range~24-41 μeV(5.8-10GHz)

整体实验方案

JPA：约瑟夫森参量放大器
TWPA：行波参量放大器

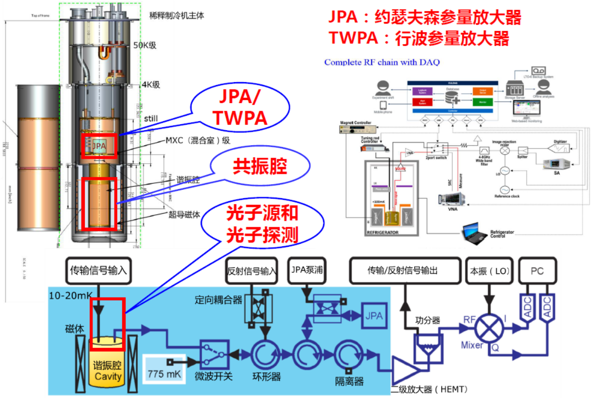

Bounds on Axion Couplings

Star	Hint ($1\,\sigma$)	Bound ($2\,\sigma$)
Sun	–	$g_{a\gamma} \leq 2.7 \times 10^{-10}\,\text{GeV}^{-1}$
WDLF	$g_{ae} = 1.5^{+0.3}_{-0.5} \times 10^{-13}$	$g_{ae} \leq 2.1 \times 10^{-13}$
WDV	$g_{ae} = 2.9^{+0.6}_{-0.9} \times 10^{-13}$	$g_{ae} \leq 4.1 \times 10^{-13}$
RGB Tip	$g_{ae} = 1.4^{+0.9}_{-1.3} \times 10^{-13}$ (M3+M5)	$g_{ae} \leq 3.1 \times 10^{-13}$ (M3+M5)
	–	$g^S_{ae} \leq 0.7 \times 10^{-15}$; $g^S_{aN} \leq 1.1 \times 10^{-12}$
HB	$g_{a\gamma} = (0.3 \pm 0.2) \times 10^{-10}\,\text{GeV}^{-1}$	$g_{a\gamma} \leq 0.65 \times 10^{-10}\,\text{GeV}^{-1}$
	–	$g^S_{ae} \leq 3 \times 10^{-15}$; $g^S_{aN} \leq 6 \times 10^{-12}$
SN 1987A	–	$g^2_{an} + 0.29\,g^2_{ap} + 0.27\,g_{an}\,g_{ap} \lesssim 3.25 \times 10^{-18}$
	–	$g_d \lesssim 4 \times 10^{-9}\,\text{GeV}^{-2}$ ($\Rightarrow f_a \gtrsim 9 \times 10^5$ GeV)
NS in CAS A	–	$g^2_{ap} + 1.6\,g^2_{an} \lesssim 1.1 \times 10^{-18}$
NS in HESS J1731-347	–	$g_{an} \leq 2.8 \times 10^{-10}$
Black Holes	–	$f_a \leq 6 \times 10^{17}\,\text{GeV}$ or $f_a \geq 10^{19}\,\text{GeV}$

Table 3: Summary of stellar hints and bounds on axions. The hints are all at 1σ and the bounds at 2σ, except for the case of SN 1987A and NS in CAS A, for which a confidence level was not provided. We have not reported the hint from the NS in CAS A [432] since it is in tension with the more recent bound in [429].

Coupling	Source	Probes	Notes
$g_{a\gamma}$	Astro	Sun	$g_{a\gamma} \leq 2.7 \times 10^{-10}\text{GeV}^{-1}$ for m_a up to a few keV
		HB-stars	$g_{a\gamma} \leq 0.65 \times 10^{-10}\text{GeV}^{-1}$ for m_a up to a few 10 keV
		SN 1987A	$g_{a\gamma} \lesssim 6 \times 10^{-9}\text{GeV}^{-1}$ for $m_a \lesssim 100$ MeV
			$g_{a\gamma} \lesssim 5.3 \times 10^{-12}\text{GeV}^{-1}$ for $m_a \lesssim 4.4 \times 10^{-10}$ eV
	Cosmo	ADMX	$m_a \sim 2 - 3.5\mu\text{eV}$. DFSZ for $m_a \sim 3\mu\text{eV}$
		HAYSTACK	$g_{a\gamma} \sim (2-3) \times 10^{-10}\text{GeV}^{-1}$ for $m_a \sim (23-24)\mu\text{eV}$
		MADMAX	DFSZ for $m_a \sim 0.04 - 0.4\text{meV}$ (*expected*)
		CULTASK	DFSZ for $m_a \sim 3 - 12\mu\text{eV}$ (*expected*, CAPP 12-TB)
			KSVZ ($E/N = 0$) for $m_a \sim 3 - 40\mu\text{eV}$ (*expected*, CAPP 25-T)
		KLASH	$g_{a\gamma} \sim 3 \times 10^{-16}\text{GeV}^{-1}$ for $m_a \sim 0.3 - 1\mu\text{eV}$ (*expected*, *Ph. 3*)
		ABRACADABRA	$m_a \sim 2.5 \times 10^{-15} - 4 \times 10^{-7}\text{eV}$ (*expected*).
			DFSZ for $m_a \sim 40 - 400\text{neV}$ (*expected*, ABRA res, *Ph. 1*)
		Radio astronomy	DFSZ for $m_a \sim 0.2 - 20\mu\text{eV}$ (*expected*)
	Sun	CAST	$g_{a\gamma} = 0.66 \times 10^{-10}\text{GeV}^{-1}$ for $m_a \lesssim 20\text{meV}$
		BabyIAXO	$g_{a\gamma} = 0.15 \times 10^{-10}\text{GeV}^{-1}$ for $m_a \lesssim 10\text{meV}$ (*expected*)
			DFSZ for $m_a \sim 60 - 200\text{meV}$ (*expected*)
		IAXO	$g_{a\gamma} = 4.35 \times 10^{-12}\text{GeV}^{-1}$ for $m_a \lesssim 10\text{meV}$ (*expected*)
			DFSZ for $m_a \gtrsim 8\text{meV}$ (*expected*)
	Lab	PVLAS	$10^{-7}\text{GeV}^{-1} \lesssim g_{a\gamma} \lesssim 10^{-6}\text{GeV}^{-1}$ for $m_a \sim 0.5 - 10\text{meV}$
		OSQAR	$g_{a\gamma} \simeq 4 \times 10^{-8}\text{GeV}^{-1}$ for $m_a \lesssim 0.4\text{meV}$
		ALPS II	$g_{a\gamma} \simeq 2 \times 10^{-11}\text{GeV}^{-1}$ for $m_a \lesssim 60\mu\text{eV}$ (*expected*)

g_{ae}	Astro	RGB-stars	$g_{ae} \leq 3.1 \times 10^{-13}$ for m_a up to a few 10 keV
		WDs	$g_{ae} \leq 2.1 \times 10^{-13}$ for m_a up to a few keV
	Sun	LUX	$g_{ae} \leq 3.5 \times 10^{-12}$
		XENON100	$g_{ae} \leq 7.7 \times 10^{-12}$
		PandaX-II	$g_{ae} \leq 4 \times 10^{-12}$
		LZ	$g_{ae} \leq 1.5 \times 10^{-12}$
		DARWIN	$g_{ae} \leq 1 \times 10^{-12}$
$g_{a\gamma} g_{ae}$	Sun	helioscopes (CAST, LUX,...)	Depends on explicit values of $g_{a\gamma}$ and g_{ae}. Can be extracted from Eq. (244) and Eq. (247)
g_{an}	Astro	SN 1987A, NS	$g_{an} \leq 2.8 \times 10^{-10}$ (from NS in HESS J1731-347)
	Lab	ARIADNE	measures $g^S_{aN} g_{an}$ down to DFSZ for $m_a \sim 0.25 - 4$meV (*expected for most optimistic choice* $g^S_{aN} = 10^{-12}$GeV$/f_a$ [482]).
		CASPEr wind	From $m_a \simeq 3.6 \times 10^{-12}$eV ($g_{an} \simeq 1.1 \times 10^{-14}$) and $m_a \simeq 9.5 \times 10^{-7}$eV ($g_{an} \simeq 5.1 \times 10^{-12}$) (*expected, Ph. 2*).
g_{ap}	Astro	SN 1987A	$g_{ap} \lesssim 3.3 \times 10^{-9}$ for $g_{an} = 0$ (hadronic axions).
g_d	Astro	SN 1987A	$g_d \leq 3 \times 10^{-9}$ GeV^{-2}
	Lab	CASPEr electric	QCD axion for $\log\left(\frac{m_a}{\text{eV}}\right) \simeq -11^{+0.8}_{-0.9}$ (*expected, Ph. 2*)

Outline

Explanation of the XENON1T Excess

- The solar axion model has a 3.5 significance, and a three-dimensional 90% confidence surface is inscribed in the cuboid defined by $g_{\mathrm{ae}} \leq 3.7 \times 10^{-12}$, $g_{\mathrm{ae}} g_{\mathrm{an}}^{\mathrm{eff}} \leq 4.6 \times 10^{-18}$, and $g_{\mathrm{ae}} g_{\mathrm{a}\gamma} \leq 7.6 \times 10^{-22}\ \mathrm{GeV}^{-1}$, and exclude either $g_{\mathrm{ae}} = 0$ or $g_{\mathrm{ae}} g_{\mathrm{a}\gamma} = g_{\mathrm{ae}} g_{\mathrm{an}}^{\mathrm{eff}} = 0$.
- Question: how to evade the cooling constraints?

Solution to the Cooling Problem [9]

- The axion couples to the photon and dark $U(1)_B$ gauge boson.

$$\mathcal{L} \supset -\frac{1}{2} g_{a\gamma A'} F'_{\mu\nu} \widetilde{F}^{\mu\nu} + g_B A'_\mu J_B^\mu \ .$$

- If the axion interactions are all assisted with ultralight dark matter ϕ, the bounds can be weakened

$$\mathcal{L} \supset -\frac{\phi}{\Lambda_e} \frac{\partial_\mu a}{2m_e} \bar{e} \gamma^\mu \gamma_r e - \frac{\phi}{\Lambda_\gamma^2} a F_{\mu\nu} \widetilde{F}^{\mu\nu} \ .$$

[9] C. Gao, J. Liu, L. T. Wang, X. P. Wang, W. Xue and Y. M. Zhong, [arXiv:2006.14598 [hep-ph]].

Axion-Like Particles (ALPs) [10]

- Lagrangian is

$$\mathcal{L}_{\text{ALP}} = \frac{g_{a\gamma\gamma}}{4} a F_{\mu\nu} \tilde{F}^{\mu\nu} + \frac{g_{aee}}{2m_e} \partial_\mu a \bar{e} \gamma^\mu \gamma_5 e \ .$$

- The ALP can be absorbed inside the detector material leading to an ioniziation signal. The cross section via the axio-electric (AE) effect is

$$\sigma_{\text{AE}}(\omega_a) = \sigma_{\text{PE}}(\omega_a) \frac{3g_{aee}^2}{16\pi\alpha_{\text{EM}} v_a} \frac{\omega_a^2}{m_e^2} \left(1 - \frac{1}{3} v_a^{2/3}\right) \ .$$

[10] I. M. Bloch, A. Caputo, R. Essig, D. Redigolo, M. Sholapurkar and T. Volansky, [arXiv:2006.14521 [hep-ph]].

The ALP Couplings

- The low energy ALP Couplings

$$g_{a\gamma\gamma} = \frac{\alpha_{\rm EM}}{2\pi f_a} E_{\rm eff} \qquad , \qquad g_{aee} = \frac{m_e}{f_a} C_{\rm eff} \,.$$

- The relations between the UV and IR ALP couplings

$$E_{\rm eff} = E_{\rm UV} + C_{\rm UV} \mathcal{A}(x) \,.$$

Here $C_{\rm UV}$ is the UV coupling of the axion to electrons, while $E_{\rm UV}$ is the UV anomaly with respect to electromagnetism, which is model dependent. $\mathcal{A}(x)$ parametrizes the electron loop function, $\mathcal{A}(x) = x \arctan^2 \frac{1}{\sqrt{x-1}} - 1$ with $x = 4m_e^2/m_a^2 - i\epsilon$ which decouples as m_a^2/m_e^2 for $m_a \ll m_e$.

The ALP Couplings

- The relations between the UV and IR ALP couplings

$$C_{\rm eff} = C_{\rm UV} + \frac{3\alpha_{\rm EM}}{4\pi^2} E_{\rm UV} \log\left(\frac{f_a}{m_e}\right) \ .$$

- For the QCD axion, the coupling to the gluon field strength gives further contributions to the effective photon and electron couplings generated by the mixing of the axion with the QCD mesons below the confinement scale

$$E_{\rm eff} \xrightarrow{\rm QCD} E_{\rm eff} - 1.92 \ , \quad C_{\rm eff} \xrightarrow{\rm QCD} C_{\rm eff} + \frac{2}{3}\frac{4m_d + m_u}{m_u + m_d} \log\frac{\Lambda_{\rm QCD}}{m_e} \ .$$

The strong X-ray limits on $E_{\rm eff}$ together with the $\mathcal{O}(1)$ contribution from QCD explains why QCD axion DM must be tuned to address the anomaly.

The Axion Models

- **DFSZ models**, where naturally $C_{\rm UV} \sim E_{\rm UV} \sim \mathcal{O}(1)$
- **KSVZ models**, where $C_{\rm UV} = 0$, and the electron coupling is only generated from the photon coupling via the running.
- **Photophobic models** where $E_{\rm eff} = 0$ and the electron coupling dominates the phenomenology.

In the absence of tuning, only the Photophobic ALP dark matter can fit the XENON1T excess without being excluded.

The ALP Dark Matter

- The best fit is

$$m_a = 2.5 \text{ keV}\,, \;\; g_{aee} = 2.5\times 10^{-14}\,, \;\; 2\log(\mathcal{L}(S+B)/\mathcal{L}(B)) = 15.7\,.$$

- If the coupling to photons is non-vanishing, the ALP DM with the desired range of masses and decay constants is severely challenged by its large decay rate into di-photons

$$\Gamma_{\gamma\gamma} = \frac{g^2_{a\gamma\gamma}}{16\pi} m_a^3\,.$$

- Imposing that the ALP is stable on timescales of our Universe gives

$$\frac{E_{\rm eff}}{C_{\rm eff}} \lesssim 38 \left(\frac{2.6 \text{ keV}}{m_a}\right)^{3/2} \left(\frac{2.7\times 10^{-14}}{g_{aee}}\right)\,.$$

The ALP Dark Matter

- A very conservative bound can be extracted by requiring the intensity of the photon line to be less than the measured CXB background at that frequency, which is $\nu_a I_{\nu_a} \simeq (2.3 \pm 0.2) \times 10^{-11}$ W m^{-2} rad^{-1}. Using this procedure, we find

$$\frac{E_{\rm eff}}{C_{\rm eff}} \lesssim 2.9 \times 10^{-3} \left(\frac{2.6 \text{ keV}}{m_a}\right)^{3/2} \left(\frac{2.7 \times 10^{-14}}{g_{aee}}\right) .$$

- A very small $E_{\rm eff}$ value is needed to explain the XENON1T anomaly, disfavoring most existing ALP models, and in particular the QCD axion, and hinting towards photophobic ALPs such as the Majoron.

The ALP Dark Matter

- For the Majoron, the XENON1T signal is correlated with possible future signals in $\mu^+ \to e^+ + a$ which could be seen at future high intensity muon facilities like Mu3e. Depending on the final seesaw scale one could further explore the parameter space looking at $\mu \to e\gamma$ at MEGII.

The Solar ALPs

- The best fit points for γ-phobic and γ-philic are respectively

$$m_a = 1.3 \text{ keV} \; , \quad g_{aee} = 3 \times 10^{-12} \; , \quad 2\log(\mathcal{L}(S+B)/\mathcal{L}(B)) = 11 \; ,$$
$$m_a = 0 \; , \quad g_{a\gamma\gamma} g_{aee} = 4.3 \times 10^{-22} \; , \quad 2\log(\mathcal{L}(S+B)/\mathcal{L}(B)) = 6.8 \; .$$

- The solar axion explanation to the XENON1T excess is in severe tension with stellar cooling constraints.

The Cooling Constraints

Star	g_{aee} bound	$\rho_{\rm core}(\text{MeV}^4)$	$T_{\rm core}(\text{keV})$
RG	4.3×10^{-13}	4.3	8.6
WD	2.8×10^{-13}	7.7	0.8
HB	9.5×10^{-13}	4.3×10^{-2}	8.6
Sun	2.4×10^{-11}	6.7×10^{-4}	1.3

Table : Summary of the bounds on the electron coupling g_{aee} from star cooling with the rough value of the density at the core.

The Cooling Constraints

- For the axion-electron coupling, g_{aee}, four stellar cooling bounds may need to be addressed: RG, WD, HB stars, and Sun cooling.
- Among the four, the solar cooling bound is the least constraining and does not exclude the ALP explanation of the XENON1T anomaly. The HB bound is in marginal tension with the XENON1T explanation if one accounts for the potentially large systematical uncertainties.
- One needs to evade the RG and WD bounds.

The Cooling Constraints

Idea: the energy losses in RG and WD are dominated by the production of light bosons in the highly degenerate core, where the central density is of order $\rho_{\mathrm{WD,RG}} \sim \mathrm{MeV}^4$, about four orders of magnitude larger than the core density of the Sun. Therefore, a model, which suppresses production only in high density stars while keeping it unaltered in low density ones, may evade RG and WD constraints and simultaneously leave the ALP production in the Sun unchanged.

The Chameleon-like ALPs

- We introduce a complex SM singlet S charged under a $U(1)_{PQ}$ symmetry, and a real SM-singlet X. The two fields are odd under the same $\mathbb{Z}_2$, and X couples to density. Below a given cutoff scale, M, we assume that the following $\mathbb{Z}_2$-invariant interactions are generated

$$\mathcal{L} \supset c_{ee} \frac{XS}{M^2} m_e e_L e_R + \frac{1}{2}\left(\frac{\rho}{M^2} - m_X^2\right) X^2 + \frac{1}{4}\lambda_X X^4 + V(S) + \text{c.c.}\,.$$

The Chameleon-like ALPs

- The potential $V(S)$ is such that S develops a VEV, $S = \frac{1}{\sqrt{2}}(f_a + s)e^{ia/f_a}$, where s is the massive singlet with mass $m_s = \sqrt{\lambda_s} f_a$ and a is the ALP, which is massless up to the addition of operators breaking the $U(1)_{PQ}$ explicitly. For $m_s \gg m_X$, we can neglect the s dynamics and write the effective coupling of the ALP to the electrons

$$g_{aee}^2 = c_{ee}^2 \frac{m_e^2}{M^2} \left(\frac{\rho - M^2 m_X^2}{\lambda M^4} \right) \Theta(-\rho + M^2 m_X^2) \ .$$

where ρ is the matter density and $\Theta(x) = 0$ if $x < 0$ and 1 otherwise.

The Chameleon-like ALPs

- The second term in the Lagrangian expresses the idea: at low densities, X has a negative mass, obtaining a VEV. Conversely, at high densities, its squared mass is positive, and the $\mathbb{Z}_2$ symmetry is restored. For $\rho \gtrsim M^2 m_X^2$, one finds $\langle X \rangle = 0$, and the coupling of the ALP, a, to electrons vanishes, shutting down its production in stars.

The Chameleon-like ALPs

- The first condition is

$$\rho_{\odot,\mathrm{core}} \lesssim m_X^2 M^2 \lesssim \rho_{\mathrm{WD,RG,HB}} \ .$$

- Second, the quartic $\lambda_{SX} X^2 |S|^2$ was omitted even though it is allowed by all symmetries. When S obtains a VEV, such a quartic induces a new mass term for X that could destroy the density-dependent VEV of X. To avoid this, we require $\lambda_{SX} f_a^2 \lesssim m_X^2$. Independently of its bare value, this quartic will be generated at one loop via the electrons. Putting all together we get an upper bound on the VEV of S

$$f_a \lesssim 24.6 \text{ MeV} \left(\frac{1}{c_{ee}}\right) \left(\frac{\rho_{\mathrm{core}}}{1 \text{ MeV}^4}\right) \ .$$

The Chameleon-like ALPs

- Third we want to explain the XENON1T excess with the cALP. Using a benchmark the solar ALP best-fit model, we get

$$c_{ee} = 5 \times 10^{-12} \lambda_X^{1/2} \left(\frac{g_{aee}}{2.6 \times 10^{-12}} \right) \left(\frac{M}{\text{MeV}} \right)^3 \left(\frac{\text{MeV}}{\rho_{\text{core}}} \right)^{1/2} .$$

- Requiring $c_{ee} \lesssim 1$ to comply with perturbativity, we get an upper bound on the cutoff scale M

$$M \lesssim M_{\text{max}} \equiv 6 \text{ GeV} \left(\frac{\rho_{\text{core}}}{1 \text{ MeV}} \right)^{1/6} \left(\frac{1}{\lambda_X} \right)^{1/6} .$$

The Chameleon-like ALPs

- Finally, we need to avoid the phenomenological constraints on X. In the limit $m_s \gtrsim m_X$ the coupling of the chameleon field X to electrons $g_{Xee} = \langle S \rangle m_e c_{ee}/M^2$ is enhanced compared to the one of the ALP and is bounded from below by

$$g_{Xee} \gtrsim g_{Xee}^{\rm min} \equiv g_{aee} \left(\frac{\lambda_X}{\lambda_s} \right)^{1/2} .$$

- Requiring $g_{Xee}^{\rm min}$ to satisfy stellar cooling constraints, and setting g_{aee} to the XENON1T best fit and $\lambda_s = 1$, we get the maximal value of $\lambda_X^{\rm max}$ allowed by stellar cooling constraints for mass range 10^{-4} keV $\lesssim m_X \lesssim 10$ keV via the RG bounds

$$\lambda_X \lesssim \lambda_X^{\rm max} \equiv 7 \times 10^{-8} \left(\frac{2.6 \times 10^{-12}}{g_{aee}} \right)^2 \left(\frac{g_{Xee}}{6.7 \times 10^{-16}} \right)^2 \left(\frac{\lambda_s}{1} \right) .$$

The Chameleon-like ALPs

- The above reveals a hierarchy between the quartic of the PQ-breaking field λ_S, and that of the chameleon, λ_X, needed in order to make this model phenomenologically viable. This hierarchy might be difficult to realize quantum mechanically.

The Chameleon-like ALPs could evade stellar cooling bounds.

Summary

- The Peccei-Quinn mechanism provides the best solution to the strong CP problem.
- It predicts axion, which can be a cold dark matter candidate.
- Axion and ALPs have deep connections to supersymmetry, grand unified theory, string theory, inflation, as well as dark energy, dark matter, the SM fermion masses and mixings, gravitational wave, baryon asymmetry, relaxation mechanism, etc, and provide explanations to the EDGES results and XENON1T excess, etc. Thus, axion and ALPs are the promising new physics beyond the SM.
- How to probe axion and ALPs at the current and future experiments?

Thank You Very Much for Your Attention!

Inflation: Standard Big Bang Cosmology Problems

- Horizon.
- Flatness.
- Initial conditions.
- Monopole.

The Cauchy Problem of the Universe: Initial Homogeneity and Initial Velocities.

Slow-Roll Parameters

For a generic inflaton potential $V(\phi)$, we have

$$\epsilon = \frac{M_{\rm Pl}^2 (V')^2}{2V^2} ~,~ \eta = \frac{M_{\rm Pl}^2 V''}{V} ~,~ \xi^2 = \frac{M_{\rm Pl}^4 V' V'''}{V^2} ~,$$

$$\sigma^3 = M_{\rm Pl}^6 (V')^2 V''''/V^3 ~,~ \delta^4(\phi) = M_{\rm Pl}^8 (V')^3 V'''''/V^4 ~,$$

$$\gamma^5 = M_{\rm Pl}^{10} (V')^4 V''''''/V^5 ~,~ \omega^6 = M_{\rm Pl}^{12} (V')^5 V'''''''/V^6 ~,$$

where $M_{\rm Pl}$ is the reduced Planck scale and $X' \equiv dX(\phi)/d\phi$.

Inflationary Observables

- The scalar spectral index

$$n_s = 1 + 2\eta - 6\epsilon \ .$$

- The running of the scalar spectral index

$$\alpha_s = 16\epsilon\eta - 24\epsilon^2 - 2\xi^2 \ .$$

- The tensor-to-scalar ratio

$$r = 16\epsilon \ .$$

- The power spectrum

$$P_s = \frac{V}{24\pi^2\epsilon} \ .$$

Inflation

- The number of e-folding

$$N(\phi) \;=\; \int_{t_i}^{t_e} H dt \approx \frac{1}{M_{\rm Pl}^2} \int_{\phi_e}^{\phi_i} \frac{V(\phi)}{V_\phi(\phi)} d\phi = \frac{1}{\sqrt{2}\, M_{\rm Pl}} \int_{\phi_e}^{\phi_i} \frac{d\phi}{\sqrt{\epsilon(\phi)}} ~.$$

- The Lyth bound

$$\Delta\phi \equiv \left|\phi_i - \phi_e\right| > \sqrt{2\epsilon_{\rm min}} N(\phi) M_{\rm Pl} ~.$$

For $r = 0.01$, 0.05, 0.1, 0.16, and 0.21, we obtain the large field inflation due to $\Delta\phi > 1.77\ M_{\rm Pl}$, 4.0 $M_{\rm Pl}$, 5.6 $M_{\rm Pl}$, 7.1 $M_{\rm Pl}$, and 8.1 $M_{\rm Pl}$ for $N(\phi) = 50$, respectively.

The Experimental Results

From the Planck, Baryon Acoustic Oscillations (BAO), and BICEP2/Keck Array data [11], we obtain

$$n_s = 0.968 \pm 0.006 \ , \ \ r = 0.028^{+0.026}_{-0.025} \ ,$$
$$\alpha_s = -0.003 \pm 0.007 \ , \ \ P_s = 2.20 \times 10^{-9} \ .$$

[11] P. A. R. Ade *et al.* [Planck Collaboration], Astron. Astrophys. **594**, A20 (2016) [arXiv:1502.02114 [astro-ph.CO]]; P. A. R. Ade *et al.* [BICEP2 and Keck Array Collaborations], Phys. Rev. Lett. **116**, 031302 (2016) [arXiv:1510.09217 [astro-ph.CO]].

The Slow-Roll Inflation

- The problems: high dimensional operators ($\phi^n V(\phi)/M_{\rm Pl}^n$) and quantum corrections.
- Why these potentially dangerous corrections are suppressed or forbidden?
- Supersymmetry is not sufficient to protect slow-roll inflation from radiative corrections because it is broken by the inflationary background at the Hubble scale.
- The only symmetry that can forbid such corrections is a shift symmetry, *i.e.*, the action is invariant under a transformation $\phi \to \phi + c$. A field possessing this symmetry (at least to some approximate level) as an axion. But how about quantum gravity effects?

Peccei–Quinn Mechanism

- The axion solution can be stabilized by the gauged discrete PQ symmetry from the breaking of an anomalous gauged $U(1)$ symmetry in string models [12].

[12] Barger, Chiang, Jiang, and TL

The Natural Inflation

- The inflaton potential

$$V = \Lambda^4 \left[1 - \cos\left(\frac{\phi}{f}\right)\right] .$$

- f can be larger than the reduced Planck scale.
- Question: how to realize it in string models?

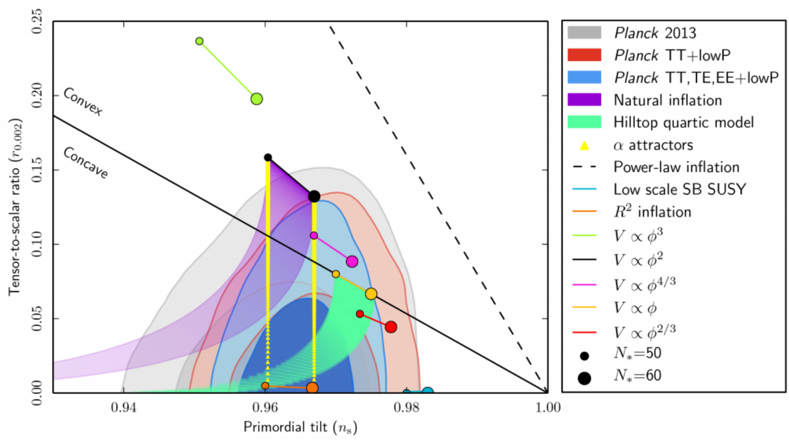

Fig. 12. Marginalized joint 68 % and 95 % CL regions for n_s and $r_{0.002}$ from *Planck* in combination with other data sets, compared to the theoretical predictions of selected inflationary models.

The Kim-Nilles-Peloso (KNP) Alignment Mechanism [14]

- Two-field inflationary potential

$$V(\phi_1, \phi_2) = \sum_{i=1}^{2} \Lambda_i \left(1 - \cos\left[\frac{\phi_1}{f_i} + \frac{\phi_2}{g_i}\right]\right) \ .$$

- The determinant of the Hessian of this potential [13]

$$\mathrm{Det}\,(V_{ij}) = \frac{(f_2\, g_1 - f_1\, g_2)^2\, \prod_{i=1}^{2} \Lambda_i\, \cos\left[\frac{\phi_1}{f_i} + \frac{\phi_2}{g_i}\right]}{f_1^2\, f_2^2\, g_1^2\, g_2^2} \ .$$

[13] X. Gao, T. Li and P. Shukla, JCAP **1410**, 048 (2014) [arXiv:1406.0341 [hep-th]].

[14] J. E. Kim, H. P. Nilles and M. Peloso, JCAP **0501**, 005 (2005) [hep-ph/0409138].

The Kim-Nilles-Peloso (KNP) Alignment Mechanism

- It will have a flat direction if the following condition holds

$$\frac{f_1}{f_2} = \frac{g_1}{g_2} \ .$$

- A small enough deviation from this condition can create a mass hierarchy between the two axions rotated in a new basis.

- Rotation of axions

$$\psi_1 = \frac{g_1 \, \phi_1 + f_1 \, \phi_2}{\sqrt{f_1^2 + g_1^2}} \, , \quad \psi_2 = \frac{f_1 \, \phi_1 - g_1 \, \phi_2}{\sqrt{f_1^2 + g_1^2}} \ .$$

The Kim-Nilles-Peloso (KNP) Alignment Mechanism

- The potential becomes

$$V(\psi_1, \psi_2) = \Lambda_1 \left(1 - \cos\left[\frac{\psi_1}{f_1'}\right]\right) + \Lambda_2 \left(1 - \cos\left[\frac{\psi_1}{f_2'} + \frac{\psi_2}{f_{\text{eff}}}\right]\right) ,$$

$$f_1' = \frac{f_1\, g_1}{\sqrt{f_1^2 + g_1^2}} , \quad f_2' = \frac{f_2\, g_2 \sqrt{f_1^2 + g_1^2}}{f_1\, f_2 + g_1\, g_2} , \quad f_{\text{eff}} = \frac{f_2\, g_2 \sqrt{f_1^2 + g_1^2}}{|f_1\, g_2 - g_1\, f_2|} .$$

- If the deviation from the flatness condition is small enough, one can generate an 'effectively' large decay constant for ψ_2 combination.

The Kim-Nilles-Peloso (KNP) Alignment Mechanism

- With an appropriate hierarchy $\Lambda_2 \ll \Lambda_1$, we can make the field ψ_1 heavier than ψ_2 with the respective masses at the minimum given as

$$m_{\psi_1}^2 \simeq \Lambda_1 \left(\frac{1}{f_1^2} + \frac{1}{g_1^2} \right), \quad m_{\psi_2}^2 \simeq \frac{\Lambda_2 \left(f_2\, g_1 - f_1\, g_2 \right)^2}{g_2^2\, f_2^2\, \left(f_1^2 + g_1^2 \right)} \ .$$

- Stabilizing ψ_1 at one of its minimum $\overline{\psi_1} = 0$ would result in a single axion potential with large decay constant

$$V(\psi_2) = \Lambda_2 \left(1 - \cos \left[\frac{\psi_2}{f_{\rm eff}} \right] \right) \ .$$

The Kim-Nilles-Peloso (KNP) Alignment Mechanism

- We successfully embed the Kim-Nilles-Peloso (KNP) alignment mechanism for enhancing the axion decay constant in the context of large volume type IIB orientifolds [15].

[15] X. Gao, T. Li and P. Shukla, JCAP **1410**, 048 (2014) [arXiv:1406.0341 [hep-th]].

The Multi-Natural Inflation [16]

- The inflaton potential

$$V(\phi) = C - \Lambda_1^4 \cos\left(\frac{\phi}{f_1}\right) - \Lambda_2^4 \cos\left(\frac{\phi}{f_2} + \theta\right) \ .$$

- The parameters

$$f_1 \equiv f \ , \quad \Lambda_1 \equiv \Lambda \ , \quad f_2 = Af \ , \quad \Lambda_2^4 = B\Lambda^4 \ .$$

[16] M. Czerny and F. Takahashi, Phys. Lett. B **733**, 241 (2014) [arXiv:1401.5212 [hep-ph]]; M. Czerny, T. Higaki and F. Takahashi, JHEP **1405**, 144 (2014) [arXiv:1403.0410 [hep-ph]]; Phys. Lett. B **734**, 167 (2014) [arXiv:1403.5883 [hep-ph]].

The Multi-Natural Inflation

- The multi-natural inflation can be realized in the supergravity theory and string inspired models?
- The hilltop quartic inflation can be realized in some approximations

$$V \simeq \Lambda^4 \left(1 - \frac{\phi^p}{\mu^p} + ...\right) , \quad \text{where } p = 4 .$$

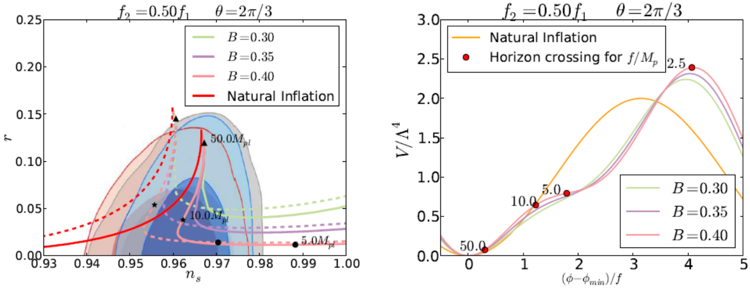

Figure 1: Left: the prediction of (n_s, r) of multi-natural inflation for three different values of Λ_2^4. Solid (dashed) lines correspond to the e-folding number $N = 60$ $(N = 50)$. Right: the corresponding inflaton potentials. The red dots represent the position at horizon crossing at $N = 60$ for the case of $B = 0.40$.

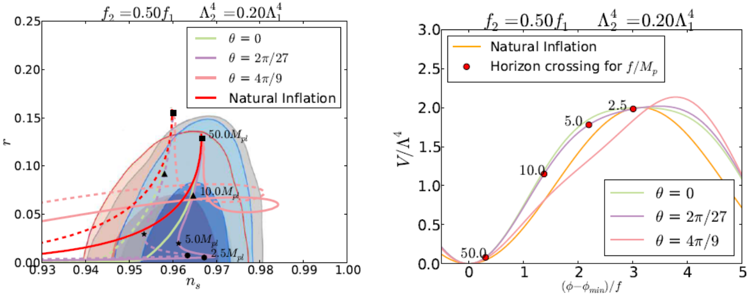

Figure 2: Same as Fig. 1 but for different values of the relative phase θ.

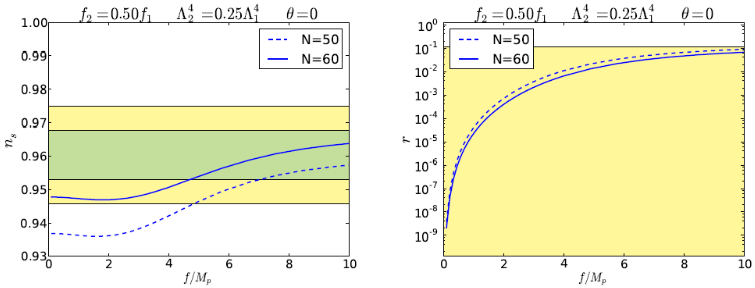

Figure 3: Behavior of n_s (left) and r (right) as a function of f. The shaded regions in the left figure correspond to 1 and 2σ allowed regions for n_s from Planck data. The shaded region on the right corresponds to the 95% CL for r ($r < 0.11$).

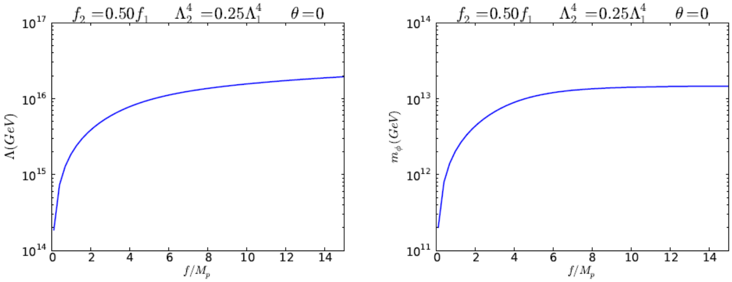

Figure 4: Planck normalized values for Λ (left) and m_ϕ (right) as a function of f.

The Axion Monodromy Inflation [17]

- The inflaton potential

$$V(\phi) = A_1 \phi^p + \sum_{i=2}^{M} A_i \cos\left(\frac{\phi}{f_i} + \theta_i\right) + V_0 \ .$$

- p is a rational number such as $p = 1$, $p = 2/3$, $p = 2$, and $p = 4/3, 3$, while M depends on the number of hidden gauge sectors which non-perturbatively generate the potential of the axion inflaton.

[17] T. Kobayashi, A. Oikawa, N. Omoto, H. Otsuka and I. Saga, Phys. Rev. D **95**, no. 6, 063514 (2017) [arXiv:1609.05624 [hep-ph]]; and references therein.

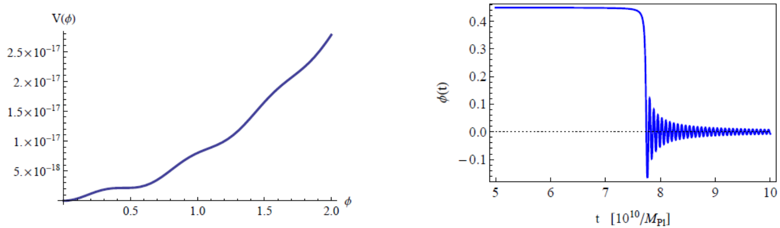

Figure 2: In the left panel, the inflaton potential is drawn by setting the parameters as $A_1/A_2 = 10.86169045$ and $A_2 = 6.30 \times 10^{-19}$, whereas the right panel shows the trajectory of the inflaton as a function of cosmic time t for the initial value of the inflaton, $\phi(0) = 0.4492824$ at $t = 0$.

N	n_s	r	m_ϕ^2	$H_{\rm inf}$	$V_{\rm inf}^{1/4}$	$\frac{dn_s}{d\ln k}$
60.0	0.9665	6.60×10^{-11}	7.67×10^{-17}	8.46×10^{-10}	3.83×10^{-5}	-2.52×10^{-3}
50.0	0.9665	1.55×10^{-10}	1.81×10^{-16}	1.30×10^{-9}	4.74×10^{-5}	-1.64×10^{-3}

Table 2: The cosmological observables such as spectral index n_s, its running $dn_s/d\ln k$, tensor-to-scalar ratio r, Hubble scale $H_{\rm inf}$, scalar potential $V_{\rm inf}^{1/4}$ at the pivot scale and the inflaton mass m_ϕ^2 at the vacuum. The parameters are set as $A_1/A_2 = 10.86169045$ and $A_2 = 6.30\times10^{-19}$ for the e-folding number $N = 60$, whereas those are set as $A_1/A_2 = 10.86169628$ and $A_2 = 6.30\times10^{-19}$ for the e-folding number $N = 50$. The initial value of inflaton field is also set as $\phi_{\rm ini} = 0.4492824$ in both cases.

The Pure Natural Inflation [18]

- The inflaton ϕ couples to the gauge field of a pure Yang-Mills theory

$$\mathcal{L} = \frac{1}{32\pi^2} \frac{\phi}{f} \epsilon^{\mu\nu\alpha\beta} \, \mathrm{Tr} \, F_{\mu\nu} F_{\alpha\beta} \ .$$

- The conventional potential from non-perturbative instantons is

$$V(\phi) = \Lambda^4 \left[1 - \cos\left(\frac{\phi}{f}\right) \right] \ .$$

[18] Y. Nomura, T. Watari and M. Yamazaki, arXiv:1706.08522 [hep-ph].

The Pure Natural Inflation

- The cosine potential is not correct in general, as argued by Witten [19] in the large N limit [20] with the 't Hooft coupling $\lambda \equiv g^2 N$ held fixed. In particular, while the physics is periodic in ϕ with the period of $2\pi f$ (because $\theta \equiv \phi/f$ is the θ angle of the Yang-Mills theory), the multi-valued nature of the potential allows for the potential of ϕ in a single branch

$$V(\phi) = N^2 \Lambda^4 \mathcal{V}(x) \ , \quad \text{where } x \equiv \frac{\lambda \phi}{8\pi^2 N f} \ .$$

- The potential does not to respect the periodicity under $\phi \to \phi + 2\pi f$.

[19] E. Witten, Nucl. Phys. B **156**, 269 (1979); Annals Phys. **128**, 363 (1980).
[20] G. 't Hooft, Nucl. Phys. B **72**, 461 (1974).

The Pure Natural Inflation

- The invariance under the CP transformation $\phi \to -\phi$ implies that $\mathcal{V}(x)$ is a function of x^2
- $\mathcal{V}(x)$ is expected to flatten as the potential energy approaches the point of the deconfining phase transition with increasing $|\phi|$ (since the dynamics generating the potential will become weaker).
- Assuming that the potential is given by a simple power law, we thus expect $\mathcal{V}(x) \sim 1/(x^2)^p$ $(p > 0)$. This potential is singular at $x \to 0$, and a simple way to regulate it is to replace x^2 with $x^2 + \mathrm{const.}$

The Pure Natural Inflation

- The axion potential is

$$V(x) = M^4 \left[1 - \frac{1}{(1+cx^2)^p}\right] \quad (p > 0) \ .$$

- The above potential for $p = 3$ can be obtained by a holographic calculation [21] in the limit of large N and 't Hooft coupling in the type IIA string theory with N stacks of D4-branes wrapping a circle:

$$V(\phi) = M^4 \left[1 - \frac{1}{\left(1 + \left(\frac{\phi}{F}\right)^2\right)^p}\right] \ , \quad \text{where } p = 3 \ .$$

[21] S. Dubovsky, A. Lawrence and M. M. Roberts, JHEP **02**, 053 (2012) [arXiv:1105.3740 [hep-th]].

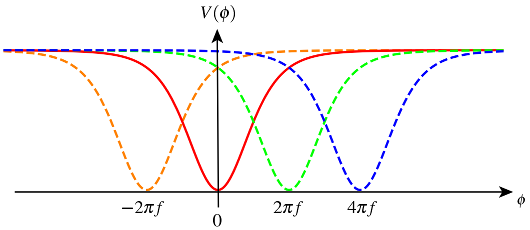

Figure : The potential of pure natural inflation (in the holographic limit $p = 3$). The potentials for other branches, which ensure the periodicity of physics under $\phi \to \phi + 2\pi f$, are also depicted by dashed lines.

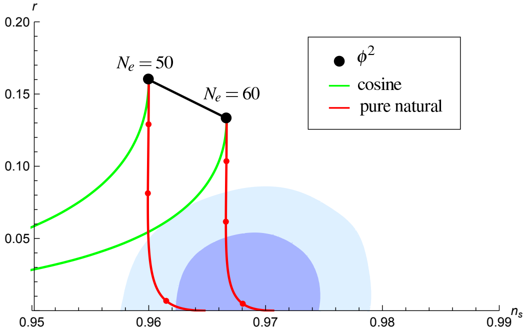

Figure : The predicted values of n_s and r superimposed with the 68% and 95% CL BICEP2/KECK Array contours. The black dots represent the predictions of the quadratic potential $V(\phi) = m^2\phi^2/2$, with e-folding $N_e = 50$ and 60. The green lines are the predictions of the cosine potential, and the red lines are those of the (holographic) pure natural inflation potential with $p = 3$. For the latter, one has varied $F/M_{\rm Pl} = 0.1 - 100$, with $F/M_{\rm Pl} = 10, 5, 1$ indicated by the red dots (from top to bottom).

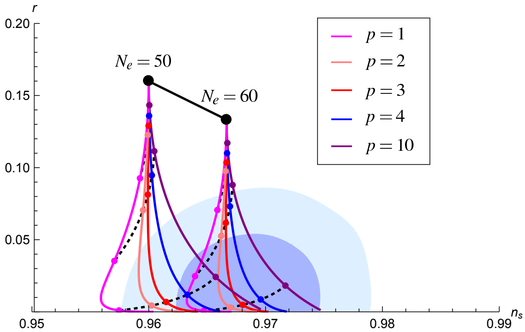

Figure : The pure natural inflation potentials with various values of $p = 1, 2, 3, 4, 10$.

The $E_8 \times E_8$ Heterotic String Theory

- The relevant Lagrangian for two form B_{MN} field

$$\mathcal{L} = \frac{3}{4}\phi^{-3/2}F_{LMN}F^{LMN} ,$$
$$H = dB + \mathrm{tr}(AF - A^3/3) + \mathrm{tr}(\omega R - \omega^3/3) .$$

- LMN are four-dimensional space-time coordinates

$$\mathcal{L} = \frac{3}{4}\phi^{-3/2}e^{6\sigma}F_{\mu\nu\rho}F^{\mu\nu\rho} .$$

- $F_{\mu\nu\rho}$ is dual to a CP-odd scalar

$$\phi^{-3/2}e^{6\sigma}F_{\mu\nu\rho} = \epsilon_{\mu\nu\rho\sigma}\partial^{\sigma}D .$$

The $E_8 \times E_8$ Heterotic String Theory

- So we have

$$dF = -\mathrm{Tr} F_{\mu\nu} \tilde{F}^{\mu\nu} + \mathrm{Tr} R_{\mu\nu} \tilde{R}^{\mu\nu} .$$

- Define dilaton field

$$S = e^{3\sigma} \phi^{-3/4} + 3i\sqrt{2} D .$$

- Thus, we have

$$\mathcal{L} = \frac{\mathrm{Im}(S)}{4} \mathrm{Tr} F_{\mu\nu} \tilde{F}^{\mu\nu} .$$

The $E_8 \times E_8$ Heterotic String Theory

- To cancel the Yang-Mills, one should introduce the Green-Schwarz term

$$\mathcal{L}_{\rm GS} = B \wedge F \wedge F \wedge F \wedge F .$$

- After compactification, we obtain

$$\epsilon^{\mu\nu\rho\sigma} F_{\mu\nu} F_{\rho\sigma} B_{ij} \langle F_{kl} \rangle \langle F_{pq} \rangle \epsilon^{ijklpq} .$$

- Thus, we obtain

$$B = \frac{1}{2\pi} \sum_{i=1}^{n} \beta_i a_i , \quad \int_{C_j} \beta_i = \delta_{ij} .$$

- Axion inflation is still consistent with the current observations.
- Axions can arise from the string theory.

Thank You Very Much for Your Attention!